ORIGINAL PAPER

Production of novel bio-transfer films composed from polyvinyl alcohol/sodium caseinate enhanced with bonded anthocyanins from poinsettia for minced meat preservation in double sheet system

Mohamed Abdin[1] · Mohamed N. Saleh[1] · Hazem Sakr[1] · Mohamed El-Bana[1] · Reham M. Kamel[2] ·
Mohamed M. El-kholy[2] · Enas El. Fadly[3] · Mohamed Abdelbaset Salama[1]

Abstract

This research explored the creation of new bio-transfer films composed of Polyvinyl alcohol (PVA), sodium caseinate (SC), and purified anthocyanin extract from poinsettia leaves (PAE). The films underwent evaluation to assess their color, physical characteristics, surface texture, crystalline structure, mechanical strength, and thermal stability. Incorporating up to 0.8% of purified anthocyanin extract (PAE) into the film matrix resulted in an opaque red color ($a* = 43.96$) and increased the opacity to 3.42 A/mm. This addition also made the films less permeable to water vapor, with a permeability rating of 1.021 ($\times 10^{-10}$ g.m^{-1} s^{-1} pa^{-1}). The film surfaces remained smooth and crack-free at lower concentrations, but became rougher when the PAE concentration reached 1.2%. Fourier transform infrared (FT-IR) analysis indicated physical interactions between the PAE extract and the Polyvinyl alcohol (PVA)/sodium caseinate (SC) matrix. These films demonstrated strong thermal stability. Furthermore, the inclusion of PAE effectively stabilized the pH, total volatile basic nitrogen (TVB-N), and peroxide value (PV) of minced meat during cold storage compared with polypropylene (PP) and un covered samples (UC), showcasing its potential as an exceptional bio-transfer medium for anthocyanins. It was recommended that the utilization of anthocyanin-based bio-transfer films not only reduce minced meat loss during storage but also promotes sustainability efforts in food preservation.

Keywords Minced meat · Bio-transfer films · Poinsettia anthocyanin extract

Introduction

The choice of materials for food packaging is crucial in maintaining food quality and safety. In response to growing environmental concerns, researchers have developed sustainable and eco-friendly biopolymer films as a viable alternative to traditional synthetic plastics. These natural materials aim to replace conventional packaging materials while minimizing their impact on the environment [1, 2]. There is a growing focus on innovative food packaging solutions that address customer concerns regarding food quality, safety, sustainability, and ecological impact. These packaging items, which include recyclable, intelligent, and multi-active options, are gaining attention as they cater to the evolving needs and anxieties of consumers [3]. Extensive research has been conducted on the utilization of natural polymers in packaging development, primarily because of their biodegradable nature and potential to reduce environmental waste. However, there is a need for further improvement in the compatibility properties of these natural polymers as compared to their synthetic counterparts. Packaging materials made from petroleum-based plastics have gained popularity due to their convenience, affordability, ease of processing, and impressive physio-chemical characteristics. Unfortunately,

✉ Mohamed Abdin
  2016208034@njau.edu.cn

✉ Mohamed Abdelbaset Salama
  Mohammed_Alsidahmadsalamp5@agr.kfs.edu.eg

1 Agricultural Research Center, Food Technology Research
   Institute, Giza 12611, Egypt

2 Agricultural Engineering Research Institute, Agricultural
   Research Center, Giza 12611, Egypt

3 Dairy Sciences Department, Faculty of Agriculture,
   Kafrelshiekh University, Kafr El-Sheikh, Egypt

the worldwide shift towards single-use plastics in modern lifestyles has resulted in packaging becoming the largest market for plastics [4]. Therefore, it is necessary to explore suitable combinations of biopolymers along with additives to enhance their overall suitability as commercially viable packaging materials, thereby addressing the need for alternatives to conventional plastic packaging.

Polyvinyl alcohol (PVA) is a synthetic polymer that holds great potential for bioplastic applications due to its desirable characteristics. It offers water solubility, biodegradability, and resistance to oil and chemicals. PVA is stable in organic solvents, making it well-suited for various applications, including paper adhesives and packaging materials. Its production involves the hydrolysis of polyvinyl acetate, a water-soluble polymer, resulting in the formation of water-insoluble PVA [5]. The biodegradability of PVA allows it to be broken down by microorganisms, making it an environmentally sustainable choice for bioplastics. Furthermore, its resistance to oil and chemicals makes it an excellent option for applications where exposure to these substances is expected, such as paper adhesives and packaging materials [6].

Sodium caseinate (SC) has emerged as a promising contender for the production of biopolymer films and coatings. Derived from casein, a protein present in milk, SC is composed of approximately 95% protein and 5% colloidal calcium phosphate. Its remarkable film-forming properties allow for the creation of environmentally friendly films that are transparent, flexible, colorless, and odorless. These films offer great potential for a wide range of food packaging applications [7, 8]. The food industry is increasingly adopting the use of natural antioxidant substances as a growing trend for food preservation. This approach aims to reduce or eliminate the reliance on harmful synthetic additives in the preservation process. Additionally, there is a growing interest in exploring active packaging systems that incorporate natural colorants and other bio-based materials. These innovative systems offer a more sustainable and environmentally-friendly approach to preserving food products. Agricultural residues are valuable resources that can be utilized to produce bio-based packaging materials [9]. The functional attributes of smart packaging can be enhanced through the integration of bioactive compounds obtained from diverse natural sources. These compounds offer valuable properties such as antioxidants and antimicrobial effects, which have garnered significant attention [10].

Anthocyanins, a class of water-soluble flavonoids, contribute to the vibrant hues observed in various parts of plants, including leaves, flowers, and fruits. These natural pigments encompass a diverse spectrum of colors, spanning from shades of orange and deep red to vibrant purples and dark blues [11]. Biodegradable films can be enhanced with the inclusion of natural pigments like anthocyanins, leading to the attainment of desired functional properties [12]. *Euphorbia pulcherrima* (Poinsettia) is a species of shrub in the family *Euphorbiaceae*. with self-supporting growth form and simple broad leaves. In poinsettia plants, the green leaves undergo a transformation from a reddish hue to a vibrant red color. This change occurs as a result of the accumulation of anthocyanins within the vacuoles of the cells [13].

The utilization of plant anthocyanins in biodegradable films makes them effective carriers for transferring their components to food. Bio-transfer films have valuable applications in the food industry, offering enhancements to the quality and functionality of food products. Through the incorporation of bioactive components into these films, they can release specific compounds into the food, providing desired attributes like antioxidant activity or antimicrobial effects [14]. Leveraging this property is of great significance in minced meat, as it helps achieve several objectives. These include extending the shelf life of minced meat, preserving its quality by inhibiting microbial growth, enhancing its color during storage, and reducing the reliance on food preservatives. Therefore, this study aims to introduce a novel packaging method for preserving meat in cold storage for extended periods by gradually transferring beneficial plant anthocyanins to minced meat. The objective of this study is to develop a bio-transfer packaging technique that ensures satisfaction in terms of food preservation, utilizing the gradual release of functional extracts like anthocyanins to enhance the quality and shelf life of minced meat.

Materials and methods

Materials

The recently procured minced meat was acquired from a local market situated in Kafrelshiekh, Egypt. The polypropylene (PP) was sourced from the Shoman factory for plastic, located in El Dakahlia, Egypt. In this process, polyvinyl alcohol (PVA) with a CAS number of 9002-89-5 was utilized, possessing a purity of 94%, a viscosity ranging from 22 to 30 cp., and a hydrolysis level of 99-99.9 (mole %). Sodium caseinate (SC) derived from bovine milk and possessing a CAS number of 9005-46-3 was also employed in the process. The fresh leaves of the poinsettia *Euphorbia pulcherrima* plant were collected from the Agricultural Research Center farm located in Egypt. The identification process of the collected plants was carried out by the Flora and Plant Classification Research Department of the Agricultural Research Center (ARC) in Egypt, using plant descriptions from the flora of Egypt as a reference. The

components such as nutrient agar and peptone, as well as the radicals ABTS and DPPH, were sourced from Sigma Aldrich Co., Ltd., located in St. Louis, MO, USA. Additionally, the glycerol plasticizer, PVA, SC, formic acid (99%), ethanol (99.8%) and acetonitrile (99.9%) utilized in the research were acquired from Gamma Scientific Comp in Egypt.

Methods

Preparation of poinsettia anthocyanin extract (PAE)

The poinsettia leaves were collected and dehydrated by oven drier at a temperature of 50ºC for a duration of 12 h. Once dried, the leaves were ground into a fine powder. Approximately 50 g of this powder were then soaked with 1.5 L of 80% aqueous ethanol (EtOH) for a period of 10 h. During this soaking process, the pH of the solution was adjusted to 4 using hydrochloric acid (HCl) at a concentration of 1.0 M. After the soaking period, vacuum filtration was employed to remove solid particles from the solution. The remaining filtrate was then subjected to centrifugation at 5,000 rpm for a duration of 12 min at room temperature. The resulting supernatants were collected and concentrated through vacuum evaporation at a temperature of 45 °C. The concentrated extracts were then transferred to a separation funnel, and ethyl acetate was added in appropriate amounts for partitioning. This partitioning process was repeated three times and the anthocyanin extract was obtained from the bottom of the funnel. The extract was loaded onto an AXR column measuring 5×52 cm. The column was washed with 3 L of a 0.5% formic acid (FA) solution to remove strongly polar ingredients. Subsequently, the required components were eluted using an eluent composed of 70% aqueous ethanol at a flow rate of 1.5 mL/min. The obtained fractions were concentrated through rotary evaporation at a temperature of 45ºC and subjected to freeze-drying, resulting in the production of the final product known as PAE.

Identification of PAE components by HPLC/ESI-MS analysis

High-performance liquid chromatography coupled to Electrospray ionization-mass spectrometry (HPLC/ESI-MS) was conducted. The HPLC analysis was performed using an Agilent 1100 series HPLC system manufactured by Agilent Technologies, headquartered in Santa Clara, CA, USA. The system was equipped with a diode array detector and employed a gradient elution technique. The analysis was carried out on a Hypersil TM ODS C18 column with dimensions of 4.6×250 mm. The analysis involved the use of two mobile phases. Phase A consisted of a mixture of trifluoroethanoic acid (TFA) and formic acid (FA) with

equal amounts, in the form of an aqueous solution containing 0.1% TFA and 1% FA (v/v). Phase B, on the other hand, was a combination of methanol and acetonitrile in a ratio of 15:85 (v/v). To achieve the desired separation, a gradient program was implemented as follows: from 0 to 20 min, the proportion of phase B was increased from 15 to 30%; from 20 to 40 min, it was further increased to 50%; from 40 to 60 min, it reached 60%; and finally, from 60 to 80 min, it reached 70%. During the analysis, an injection volume of 20 µl was used, and the flow rate was maintained at 0.6 ml/min. The detector wavelengths were set at 280 nm and 530 nm to capture desired signals. Additionally, the column oven temperature was set at 35 °C to ensure optimal conditions for the separation process. ESI-MS data were acquired using an Agilent 6410B Mass Spectrometer equipped with electrospray ionization (ESI) in the positive ion mode. The mass spectrometer was configured with specific settings for the MS analysis. These settings included a dry gas temperature of 330 °C, a dry gas flow rate of 10 ml/min, a full scan mass range from 100 to 1000 m/z, a capillary voltage of 3.5 KV, and a nebulizer pressure of 35 psi.

Preparation of PVA/SC/PAE films

The preparation of PVA/SC/PAE films was conducted using a modified casting method [15]. In this process, 3 g of PVA were dissolved in 100 mL of distilled water at 95 °C for 30 min in a 250 mL beaker, with continuous stirring at 700 rpm. Separately, 2 g of SC were dissolved in 150 mL of distilled water at 60 °C for 40 min in a 500 mL beaker, also stirred at 700 rpm. The PVA solution was then carefully poured into the beaker with the SC solution to create a PVA/SC blend, which was stirred for an additional hour at 60 °C. During this period, 1.8 g of glycerol were incorporated into the blend. Various concentrations of lyophilized PAE were also added to achieve final concentrations of 0.4%, 0.8%, and 1.2% in the solution, creating three distinct mixtures: PVA/SC/PAE1, PVA/SC/PAE2, and PVA/SC/PAE3. Each mixture (60 mL) was then poured into 15 cm diameter petri dishes, which were placed in an air oven drier at 50 °C for 10 h to dry. After drying, the films were carefully removed from the dishes and stored in a desiccator for further analysis.

Examination of surface, cross-sectional and topography of films

The scanning electron microscope (SEM) analysis was performed to examine the surface and cross-sectional structures of the PVA/SC/PAE films. Initially, the films were cut into small square sections and dried. These sections were then mounted on metal grids using double-sided adhesive

tape to ensure stability. The next step involved coating the samples with gold particles, which were sprayed onto both the surface and cross-sections. Photographs were then taken using a scanning electron microscope (SEM) from Philips-FEI Co., AMS, based in Eindhoven, Netherlands, operating at a voltage of 5 kV and with a magnification power of 500 μm. In addition, the surface morphology of the films was analyzed using an Atomic Force Microscope (AFM) equipped with a Scanning Probe Microscopy (SPM) probe of the NanoScope MultiMode type, produced by Veeco Metrology, Inc., located in Santa Barbara, USA.

FT-IR analysis of produced PVA/SC/PAE films

The PVA/SC/PAE films underwent analysis using a Spectrum 3 Fourier transform infrared (FTIR) spectrometer manufactured by PerkinElmer in the United States. Each spectrum was captured within the range of wavenumbers from 4000 to 500 cm^{-1}, with a resolution of 5 cm^{-1}.

X-ray diffractometry properties of PVA/SC/PAE films

The X-ray diffraction (XRD) patterns of the PVA/SC/PAE films were verified using a D8 Advance X-ray diffractometer manufactured by Bruker in Germany. The XRD analysis was performed using stabilized radiation at an operating current of 40 mA and voltage of 40 kV. The scanning process covered a 2θ diffraction angle range from 5 degrees to 80 degrees, with a scanning rate of 10 degrees per minute.

Thermal properties of PVA/SC/PAE films

The simultaneous thermal analysis of Thermogravimetry was carried out using an STA-8000 thermal analyzer from PerkinElmer, located in Norwalk, CT, USA. The heating rate was set at 10 °C per minute, with the temperature range varying from 35 to 700 °C. The weight loss and thermal degradation were measured in the presence of a nitrogen atmosphere.

Characterization of mechanical properties

The mechanical properties of the PVA/SC/PAE films were assessed by measuring their tensile strength (TS) and elongation at break (EB). Briefly, the films sized at 3×12 cm^2, were securely clamped between the grips of an Instron 5567 universal testing machine, Instron Co., USA. The machine was configured with an initial grip separation of 60 mm and a cross-head speed of 140 mm/min. The determination of TS and EB was calculated as following;

$$TS\,(MPa) = \frac{Mt}{Th \times D}$$

$$EB\,(\%) = \left(\frac{Ex - Ig}{Ig}\right) \times 100$$

The peak tension experienced during the stretching process is referred to as Mt. In this context, Th represents the thickness of the films, D represents the width, Ex represents the extensibility of the film in mm, and Ig represents the initial length of the film between the grips in mm.

Determination of PVA/SC/PAE biodegradability

The biodegradability of PVA/SC/PAE films was assessed through a standardized decomposition analysis. The films, measuring 3×3 cm, were placed on soil within a tray measuring 15×15 cm, and left undisturbed for a period of 30 days. Twice daily, the soil was sprayed with water, and the weight loss during time was calculated every 5 days.

Antioxidant activity of PVA/SC/PAE films

Film weighing 50 mg were immersed in 6 mL of distilled water to fully extract the anthocyanins for subsequent analysis. For the assessment of DPPH (2,2-diphenyl-1-picrylhydrazy) radical scavenging activity, 3.0 mL of this extract was combined with 1.0 mL of a methanol solution that contained 0.1 mM DPPH. The mixture was then stored in a dark setting for 30 min. Following this period, the absorbance of the mixture was recorded at 520 nm using spectrophotometer and the DPPH scavenging activity was determined by the following equation;

$$DPPH\,radical\,scavenging\,activity\,(\%) = \left(\frac{Abs\,DPPH\,solution - Abs\,films}{Abs\,control}\right) \times 100$$

In the given equation, "Abs control" denotes the absorbance of the DPPH solution alone, without any film samples, while "Abs films" indicates the absorbance when the DPPH solution is combined with the test films. To assess the ABTS (2,2'-azino-bis (3-ethylbenzothiazoline-6-sulfonic acid) radical scavenging activity, a working solution was created by blending 145 mM potassium persulfate with 7 mM ABTS reagent. This mixture was stored in the dark for 10 h. Subsequently, the solution was diluted with 0.2 M pH 6.5 PBS to achieve an absorbance level no higher than 0.8. For the scavenging test, 30 μL of the extract from the films was mixed with 1970 μL of this working solution and incubated in dark for 30 min. The absorbance of this final mixture was

then measured at 520 nm, and the results were calculated using the provided formula.

$$ABTS \, radical \, scavenging \, activity \, (\%) = \left(1 - \frac{Abs1 - Abs2}{Abs3}\right)$$

Abs1 is the absorbance of films, Abs2 is the absorbance of samples with PBS and Abs3 is the absorbance of ABTS.

Determination of PVA/SC/PAE water contact angel

To determine the water contact angle (WCA) of the PVA/SC/PAE films, an optical contact angle HARKESPCAX1, HARKE, China was utilized. The drop methodology, as described in reference [16], was employed for this purpose. In this method, each film sample was securely placed on a glass slide using adhesive tape to ensure stability. Pure water was then carefully dropped onto the surface of the films. The shape of the water droplet was observed and recorded in order to calculate the WCA values. To ensure accuracy and reliability, this process was three four times for each sample.

Antibacterial activity of PVA/SC/PAE films

The resistance of PVA/SC/PAE films was evaluated against bacterial strains *Staphylococcus aureus ATCC 6538* and *Salmonella typhimurium ATCC 14,028*. A nutrient agar broth medium was prepared by dissolving yeast extract (2.5 g/L) and peptone (4.5 g/L) in 20 mL of solution, maintaining a pH between 6.8 and 7.2, within a conical flask. This broth was then inoculated with the bacterial strains and incubated at 37 °C for 24 h. Following incubation, the culture was centrifuged at 6000 × g for 2 min, the supernatant removed, and the bacterial pellet preserved. The pellet underwent two washes with sterile 0.85% NaCl solution. The bacterial suspension was then adjusted to a 0.5 McFarland standard optical density. Sterile circular film samples were arranged on petri dishes filled with solid medium. A 0.1 mL volume of the standardized bacterial suspension was evenly distributed over the medium around each film sample. These plates were then incubated at 37 °C for another 24 h, after which the inhibition zone diameter around each film piece was measured with a sliding caliper.

Characterization of films thickness, solubility and swelling degree

To determine the thickness of PVA/SC/PAE films, a digital micrometer (measuring range: 0–25 mm/0–1, resolution: 0.001 mm/0.0001) was employed. Small film sections were cut and positioned vertically between the micrometer's ends. Tight contact was ensured at various locations across the film. four thickness measurements were directly obtained and averaged to arrive at the final film thickness.

After a 24-hour immersion in 30 mL of distilled water, the dried films underwent a two-part analysis to determine their solubility and swelling. The insoluble film portions were separated by filtering the mixture through pre-weighed paper. One set of these filters was then re-dried at 105 °C until constant weight, establishing the "M1" value. The remaining filters were dried naturally at ambient 25 °C, providing the (M2) weight. These weights, along with the initial film mass (M0), were used to calculate solubility and swelling degree using specific equations.

$$\textbf{Solubility} \, (\%) = \left(\frac{\textbf{M}2 - \textbf{M}0}{\textbf{M}2}\right) \times 100$$

$$\textbf{Swelling degree} \, (\%) = \left(\frac{\textbf{M}2 - \textbf{M}0}{\textbf{M}0}\right) \times 100$$

Characterization of films water vapor permeability

The water vapor permeability (*WVP*) was determined according the previous method [17] with suitable modification. Briefly, a volume of 15 mL distilled water was established in conical flasks, each topped with a PVA/SC/PAE films secured by a rope. These flasks were then housed in a desiccator maintained at 50% relative humidity and 25 °C, generating a controlled water vapor pressure difference across the film. A digital gauge tracked the pressure disparity throughout the experiment. Simultaneously, the flasks' weights were recorded every 2 h for 12 h. These data points, along with the known film area and equation parameters, were then used to calculate the *WVP* of the films.

$$\textbf{WVP} = \frac{\textbf{\Delta w.f}}{\textbf{A.t.\Delta P}}$$

Δw: Change in weight of the flasks, f: Film thickness, A: Exposed area of the film, t: Time interval, ΔP: Change in water pressure.

Determination of color properties and opacity

The Konica Minolta Cr color reader was utilized to assess the color parameters L*, a*, and b*. An increase in L* suggests a trend toward greater transparency, whereas increases in a* and b* indicate shifts toward red and yellow hues, respectively. To guarantee precise measurements, the samples were placed on the machine's white board and left

to stabilize prior to recording readings from five different areas. These values were averaged to determine the mean. The total color difference, ΔE, was calculated using a designated formula.

$$\boldsymbol{\Delta E} = \sqrt{\left(\boldsymbol{\Delta L*}\right)^2 + \left(\boldsymbol{\Delta a*}\right)^2 + \left(\boldsymbol{\Delta b*}\right)^2}$$

The opacity of the films was measured using the Genesys 10 S UV-VIS ultraviolet spectrophotometer, produced by Thermo Fisher Scientific, USA. Prior to testing, the thickness of each film was measured and factored into a calculation formula to specifically assess the opacity at a wavelength of 600 nm.

$$Opacity = \frac{Ab600}{Th}$$

where Th is the films thickness (mm).

Film application as active packaging for minced meat preservation

Fresh minced meat samples, each weighing 250 g, were sandwiched between two 15 cm diameter circular film pieces made of Polypropylene (PP) and PVA/SC/PVA2. These samples were then sealed and vacuum-packed using a circular heater impulse sealer machine (Mercier Corporation, ME-455A1, Taipei, Taiwan), ensuring the edges were tightly sealed to maximize contact between the meat and the active films, as illustrated in Fig. 6D. The packaged samples were subsequently stored in a refrigerator at 5 °C for a duration of 10 days. Samples were extracted for analysis from each type of packaging on days 0, 5, and 10, with three replicates taken each time.
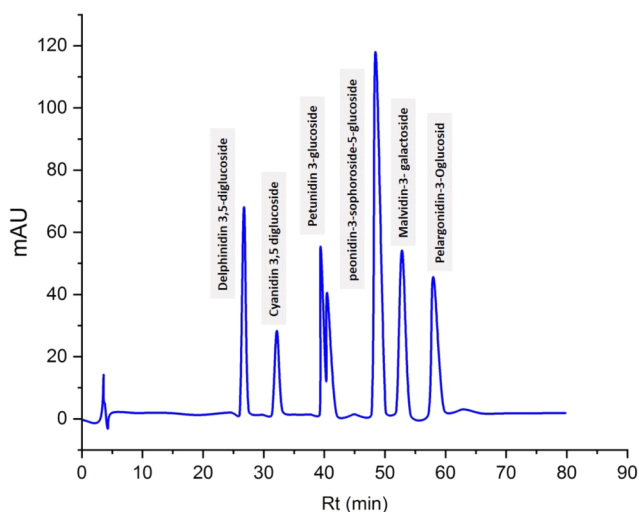

Fig. 1 HPLC chromatogram of detected PAE components

Determination of pH, TVB-N and peroxide value during storage

The determination of Total Volatile Base Nitrogen (TVB-N) content and pH levels was carried out using the standard method previously outlined by Jouki et al. [18]. Meanwhile, the procedure for measuring the peroxide value (PV) involved initially mixing 2 g of minced meat with a solution of acetic acid and chloroform in a 12:18 ratio in a vessel. Then, 1 mL of saturated potassium iodide solution was added to the blend, stirred for one minute, and left to stand in a dark place for 5 min. Subsequently, 30 mL of distilled water and 1 mL of starch indicator were added. The mixture was then titrated with a 0.01 N sodium thiosulfate solution, and the peroxide value was calculated using the specific equation provided.

$$PV = \frac{(V1 - V2) * N * 1000}{W}$$

The equation for calculating the peroxide value (PV) involves several variables. V1 represents the volume of sodium thiosulfate used to titrate the sample, while V2 represents the volume of sodium thiosulfate used to titrate the control sample. N signifies the normality or concentration of the sodium thiosulfate solution, and W represents the weight of the sample. By utilizing these variables in the provided equation, the peroxide value can be determined accurately.

Statistical analysis

Statistical analysis was conducted using SPSS version 20.0 to identify variations. The Tukey's Honest Significant Difference (HSD) test was applied to discern significant differences among the means. A p-value below 0.05 was deemed statistically significant.

Results and discussion

Analysis of purified PAE

The chromatographic finger print profiles of anthocyanins extracted from PAE, displayed in Fig. 1, reveal six distinct anthocyanin peaks using high-performance liquid chromatography (HPLC). Each peak was further analyzed using LC-MS/MS for anthocyanin identification, which was carried out based on the retention times and mass spectral data found in various libraries and referenced sources. As shown in Table 1, a range of positive molecular ion $[M]^+$ (m/z) from 433 to 787 were obtained in PAE. According to the fragment patterns and previous reports [19], cyanidin 3,5

**Table 1** Corresponding molecular mass of HPLC detected peaks

Tentative identification	RT (min)	λmax (nm)[c]	[M]⁺ (m/z)
Delphinidin 3,5-diglucoside	26.24	275, 528	627
Cyanidin 3,5 diglucoside	32.41	276, 515	611
Petunidin 3-glucoside	41.74	275, 527	479
Peonidin-3-sophoroside-5-glucoside	48.14	277, 518	787
Malvidin-3- galactoside	52.73	278, 522	630
Pelargonidin-3-oglucosid	58.09	279,525	433

di-glucoside and petunidin 3-glucoside were detected with positive molecular ion [M]⁺ 611 and 479 respectively, in anthocyanins extracts. Additionally, the attendance of delphinidin 3,5-diglucoside and peonidin-3-sophoroside-5-glucoside were proved in highly purified anthocyanins with typical positive molecular ion [20, 21]. Furthermore, malvidin-3- galactoside and pelargonidin-3-Oglucosid were noticed previously with [M]+ (m/z) 630 and 433; respectively [22, 23].

Films SEM micrographs

The surface, cross-sectional morphologies and real photos of the control (PVA/SC) and PVA/SC/PAE films were observed using SEM in Fig. 2. The irregular surface of the control films (PVA/SC) with cracks in cross sectional images were noticed. The analysis of the surface and cross-sectional morphology of PVA/SC films with different levels of purified PAE showed no significant changes at the lower concentrations (PVA/SC/PAE1 and PVA/SC/PAE2). This indicates that incorporating PAE at specific concentrations (0.8%) promoted a positive interaction and achieved good compatibility between the combined polymers. The surface and cross-sectional views of PVA/SC/PAE2 displayed a consistent shape with no cracks or agglomerations. The presence of cyanidin, malvidin and petunidin in the extract could potentially contribute to the hydrophilicity, which in turn promotes the even distribution of two colloids. This, in turn, has a positive impact on the photocatalytic properties of the films, particularly in the context of automatic food freshness monitoring [24].

Fig. 2 SEM micrographs of surface, cross sectional and AFM topography of (**A, E and I**) PVA/SC, (**B, F and J**) PVA/SC/PAE1, (**C, G and K**) PVA/SC/PAE2 and (**D, H and L**) PVA/SC/PAE3 films
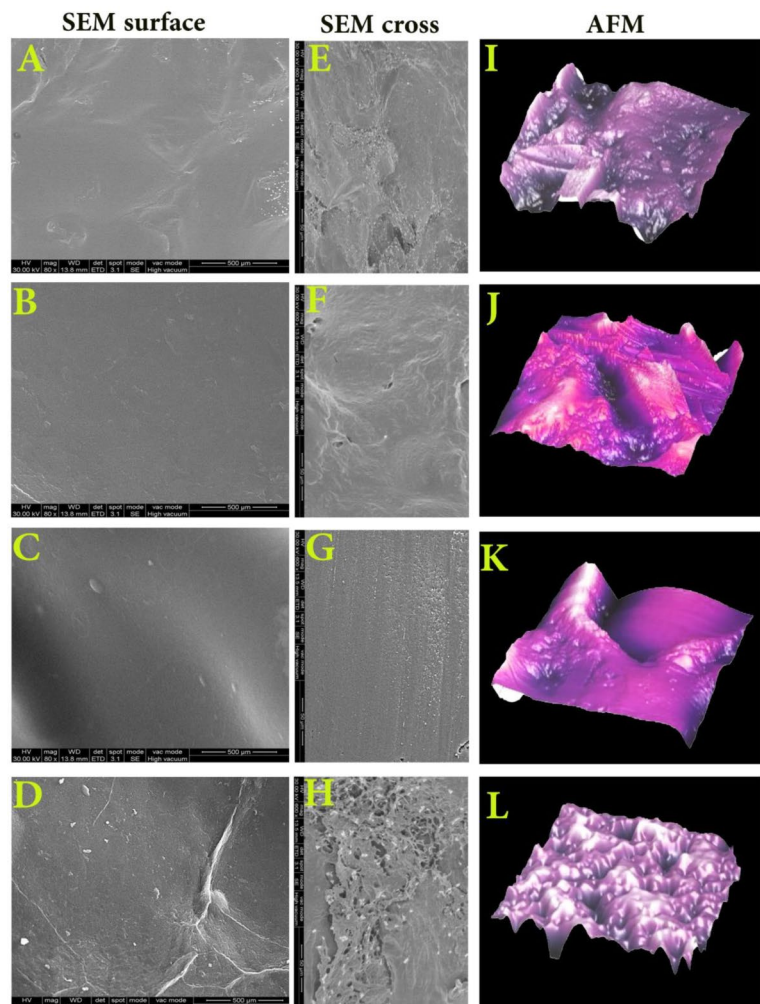
However, introducing higher concentrations (1.2%) of PAE into the PVA/SC films (PVA/SC/PAE3) led to the development of curls, a rough surface, and noticeable holes in the cross-sectional structure of the films. This irregularity could be attributed to localized microphase separation within the PVA/SC matrix due to the high levels of PAE. Similar phenomena were previously observed [15] following the addition of phenolic extract from broccoli sprout seed into films made of carboxymethyl cellulose and polyvinyl alcohol. The addition of PAE within control films led to a reduction in impedance and a decrease in topographical roughness, as depicted in Fig. 2J-K, resulting in the formation of small plateaus on the film surface. However, the incorporation of PAE within (PVA/SC/PAE2) resulted in the disappearance of these plateaus. Subsequently, a significant number of plateaus reappeared, resembling an egg box appearance, as shown in Fig. 2L. The topographical features observed aligned with the findings from the SEM analysis.

Water contact angel of PVA/SC/PAE films

The water contact angle (WCA) in films holds substantial importance across various applications. The WCA denotes the angle that materializes between the film's surface and a water droplet positioned upon it. This parameter is widely utilized for evaluating the surface's hydrophilicity or hydrophobicity. As illustrated in Fig. 3A, the PVA/SC films showed WCA at 84.32 º. The presence of PAE in PVA/SC/PAE1 and PVA/SC/PAE2 decreased the WCA to 77.80 º and 74.20 º, respectively. As the concentration of PAE increased in PVA/SC/PAE3, the WCA value decreased, eventually reaching a value of 42.6º. Anthocyanins exhibit hydrophilic properties because they are soluble in water. The inclusion of hydrophilic groups, such as hydroxyl groups, within the anthocyanin structure contributes to their water solubility. These hydrophilic groups have the ability to engage with water molecules after falling on films, thereby intensifying the hydrophilic characteristics of anthocyanins and resulting in a decrease in the WCA.

Films FT-IR analysis

To explore the interaction between the PVA/SC film matrix and PAE, FT-IR analysis was performed and illustrated in Fig. 3E. The FT-IR spectrum for the PVA sample, shown in Fig. 3A, displays a prominent, wide peak at 3265 cm^{-1}, which suggests strong hydrogen bonding associated with the hydroxyl group's stretching vibrations. Additionally, a lesser peak at 2912 cm^{-1} corresponds to the stretching vibrations of CH_2 and CH groups [15]. The spectrum also shows a peak at 1597 cm^{-1}, likely indicative of carbonyl functional groups. Peaks at 1088 and 1027 cm^{-1}, associated

with C-O stretching vibrations, are noted for their sensitivity to crystallization according to the analysis [25]. In the FT-IR spectrum of the SC sample, noticeable peaks at 3447 and 1649 cm^{-1} highlight the bending and stretching vibrations of the free hydroxyl groups -OH groups, respectively. Further, peaks at 669 cm^{-1} and 2922 cm^{-1} represent the bending and stretching vibrations of the C-H groups [7].

The combination of PVA and SC resulted in the following spectral modifications. The absorption band, ranging from 3265 to 3447 cm^{-1} and indicative of the -OH group's stretching vibrations, shows a narrower peak at 3265 cm^{-1} in the spectrum. Additionally, the peaks observed from SC between 1510 and 1649 cm^{-1}, along with the 1597 cm^{-1} peak from PVA, have converged into a single peak at 1598 cm^{-1} in the PVA/SC spectrum. The 1027 and 1088 cm^{-1} peaks from PVA have coalesced into two distinct peaks at 920 and 1110 cm^{-1} in the PVA/SC sample. Moreover, the band observed at 1022 cm^{-1} is associated with the hydroxyl group from glycerol, which was added as a plasticizer [26]. The inclusion of PAE at specific concentrations (0.4–0.8%) did not alter the profile of the PVA/SC film curves, implying that the film's matrix can accommodate anthocyanin content without undergoing any chemical modifications. This shift suggests a physical interaction between PVA/SC and PAE, effectively preserving the original active components without diminishing their bioactivity. Such an interaction has been previously documented in other studies [27]. Nonetheless, incorporating PAE at a concentration of 1.2% in PVA/SC films led to a splitting and earlier appearance of the spectral band, shifting from 3266 cm^{-1} in PVA/SC/PAE1-2 to 3251 cm^{-1} in PVA/SC/PAE3.

XRD characteristics

The X-ray diffraction (XRD) analysis was employed to ascertain the crystalline structure of both PVA/SC films devoid of extracts and PVA/SC/PAE films with varying concentrations of extracts (Fig. 3F). The XRD analysis revealed characteristic patterns for PVA/SC films, indicating a crystalline index of 44.81%. Similarly, for PVA/SC/PAE1-2 films, the crystalline indices were measured at 43.22% and 46.70% respectively. Interestingly, incorporating plant extracts at suitable concentrations into the polymer films did not alter the crystalline structure of the films [28, 29].

When higher concentrations (1.2%) of PAE were incorporated to produce PVA/SC/PAE3, noticeable changes were observed in the XRD analysis. The broad peaks in the diffraction patterns became wider and shifted to higher Bragg angles ($2\theta = 23.83º$, $32.72º$, and $43.31º$). This indicated the presence of some localized organization within the complex system. Additionally, a minor peak at 28.32º, which was present in PVA/SC and PVA/SC/PAE1-2 films, disappeared.

Fig. 3 Water contact angel of PVA/SC (**A**), PVA/SC/PAE1 (**B**), PVA/SC/PAE2 (**C**) and PVA/SC/PAE3 (**D**). FT-IR transmittance (**E**), XRD patterns (**F**), DTG analysis (**G**) and TGA thermograms (**H**) of PVA/SC, PVA/SC/PAE1, PVA/SC/PAE2 and PVA/SC/PAE3
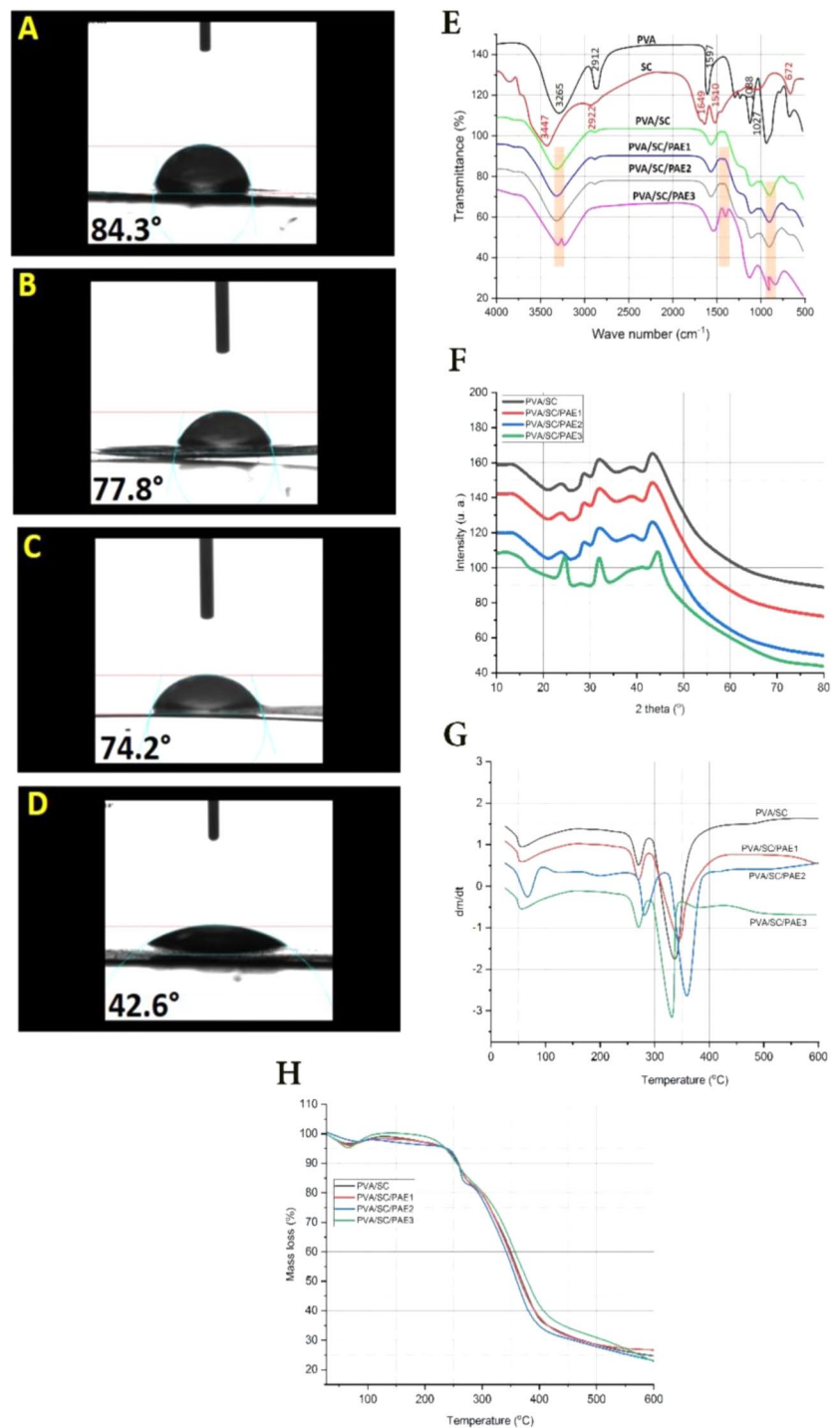
The addition of plant extracts in non-standardized amounts slightly disrupted the structural order of the sustainable films [30]. It was also noted that the height of the diffraction peaks in the films could change with the addition of plant anthocyanin extracts [31]. The degree of structural order is critical for maintaining the stability and functionality of the films. Thus, this observation underscores the need to precisely control the concentration of plant extracts during manufacturing to maintain film integrity. The X-ray diffraction (XRD) results corroborate the scanning electron microscopy (SEM) images, which show cracks on the surface of films with higher concentrations of PAE. Additionally, the XRD data help explain the observed reductions in tensile strength and elongation at break in the films. These results suggest that a high concentration of PAE compromises

the structure and physical properties of the films, leading to decreased mechanical strength and flexibility.

Thermal diagnosis of PVA/SC/PAE films

The thermal diagnosis of PVA/SC/PAE was noticed in Fig. 3G-H by DTG and TGA analysis. DTG and TGA analysis can provide insights into the thermal stability and degradation kinetics of biodegradable films. By measuring the weight loss and corresponding temperature changes, it helps determine the temperature range at which the film starts to degrade or undergo thermal decomposition [32, 33]. Three events were observed in the DTG/TGA curves of PVA/SC and PVA/SC/PAE, and they were attributed to the removal of physically absorbed water (from 25 to 70 °C) [34], the degradation of PVA or SC (from 250 to 300 °C) and the breakdown of whole composite film (from 320 to 400 °) [35]. PVA/SC/PAE2 films exhibited the highest level of thermal stability, as evidenced by the delayed breakdown process occurring at 365.21 °C, in contrast to PVA/SC films that experienced breakdown at 342.13 °C. This investigation further reinforced the superior thermal stability of the bio-composite films compared to the control films. The inclusion of anthocyanin in the PVA/SC film likely resulted in the formation of a robust PVA/SC matrix with a rigid PVA component bridging between the anthocyanin and SC molecules. Similar characteristics have been previously observed

[36]. The alterations in crystallinity and the presence of irregularities on the film surface, resulting from the addition of higher concentrations of anthocyanins, could potentially be the primary factor contributing to the decrease in thermal stability observed in PVA/SC/PAE3. This film experienced degradation at a temperature of 334.14 °C and this explanation is consistent with the XRD and SEM analysis.

Regarding TGA analysis, the study demonstrated that the weight loss in PVA/SC/PAE1-2 films was less than that in PVA/SC films, indicating that adding PAE up to a 0.8% concentration enhances the thermal stability of the film. On the other hand, PVA/SC/PAE3 films showed greater weight loss than the PVA/SC films. The weight loss trends in PVA/SC/PAE3 suggest that the higher concentration of PAE disrupts the interaction among polymer chains, thus leading to an earlier onset of decomposition. This pattern aligns with previous findings where the addition of plant extracts to polymer combinations had similar effects [27, 37].

Mechanical characteristics of PVA/SC/PAE films

The mechanical characteristics (depicted in Fig. 4A) of biodegradable films containing anthocyanins are critical for evaluating their functionality and performance. Tensile strength (TS) gauges the ability of the film to resist forces that stretch or pull it without failing structurally. Conversely, elongation at break (EB) indicates how far the film

Fig. 4 Mechanical properties (**A**), biodegradability (**B**) and antioxidant activity (**C**) of PVA/SC, PVA/SC/PAE1, PVA/SC/PAE2 and PVA/SC/PAE3
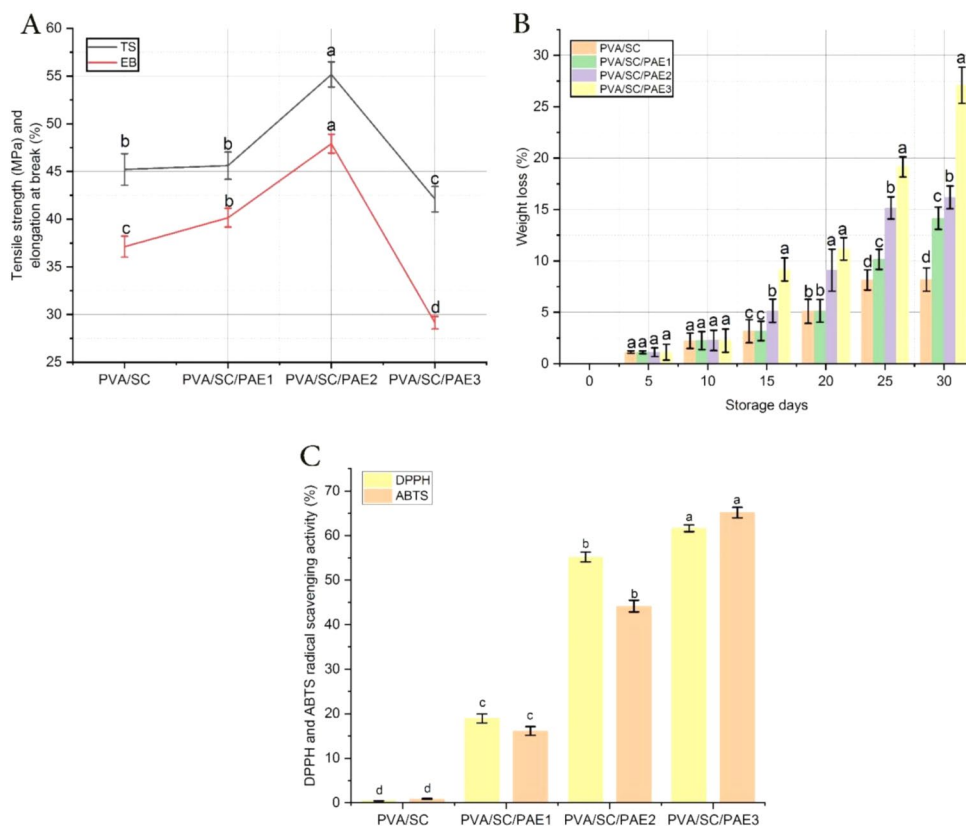
can extend or deform before it reaches its breaking point [38, 39]. As shown in Fig. 4A, the inclusion of PAE significantly enhanced ($P < 0.05$) both the tensile strength (TS) and elongation at break (EB) for PVA/SC/PAE1 and PVA/SC/PAE2 compared to the control (PVA/SC). This improvement can be attributed to the presence of glycerol and the chemical composition of PAE, which includes hydrophilic groups. These groups help achieve a more homogeneous structure in the control films (PVA/SC), promoting strong hydrogen or ionic bonding between the hydroxyl groups of the film matrix and the anthocyanin components. Additionally, the increase in EB in anthocyanin-enhanced biodegradable films suggests greater compatibility and homogeneity between the anthocyanins and the film structure, which in turn enhances molecular mobility and reduces the film's rigidity and strength [40]. Earlier research has documented enhancements in both tensile strength (TS) and elongation at break (EB) of films after the inclusion of carboxymethyl chitosan-gum arabic and anthocyanins derived from the peel waste of *Cinnamomum camphora* fruit [24]. The continual incorporation of PAE into PVA/SC films led to a deterioration in the mechanical properties of the complex structure. The observed decrease in tensile strength (TS) and elongation at break (EB) may be linked to disruptions in the intermolecular and intramolecular bonding among PVA and SC chains caused by the presence of anthocyanin molecules [41]. Furthermore, using higher concentrations of PAE in PVA/SC/PAE3 films showed alterations in the films' crystalline properties, microstructure, chemical structure, and surface uniformity, as confirmed by XRD, FT-IR, and SEM analyses. These changes significantly affect the mechanical properties of the films [42]. The appearance of cracks and wrinkles on the surface of PVA/SC/PAE3 films compromises their structural integrity, making them more prone to tearing and easier to break during stretching.

Biodegradability of PVA/SC/PAE films

The biodegradability of films can vary depending on the specific materials used, the presence of additives, and the exposure to environmental conditions. The potential biodegradation results of PVA/SC and PVA/SC/PAE films are illustrated in Fig. 4B. After being buried in soil for a duration of 5–10 days, nearly all film types exhibited a similar percentage of weight loss. However, beyond the 10-day mark, the PVA/SC/PAE1-2 film demonstrated the highest level of weight loss during the storage period. Notably, the PVA/SC/PAE2 film exhibited the most favorable degradability, with a weight loss value of 26.32% after 30 days, while the PVA/SC film had the lowest weight loss value of 8.89%.

Studies have shown that the inclusion of plant extracts in biodegradable films can expedite their breakdown in soil,

thus contributing to environmental sustainability. Similar results have been observed in research exploring the incorporation of various plant extracts into films [43, 44].

Antioxidant activity of PVA/SC/PAE films

Incorporating plant extracts into biodegradable films has been shown to have antioxidant effects. These extracts have been found to inhibit peroxide, fluorescent compound, and free fatty acid values, indicating their antioxidant activity [45]. As indicated in Fig. 4C, the results revealed that PVA/SC/PAE3 films had the highest scavenging activity for ABTS and DPPH radicals, followed by PVA/SC/PAE1 and PVA/SC/PAE2 ($p < 0.05$). Hence, it can be deduced that among the examined film samples, PVA/SC/PAE3 demonstrated the most pronounced radical scavenging activity. The research indicates that the primary factor contributing to the antioxidant properties of the films is the existence of the PAE. Anthocyanins in biodegradable films exhibit strong antioxidant properties and are recognized for their ability to scavenge free radicals. Their mechanism of action involves two proposed pathways: one involves targeting the hydroxyl group(s) on the B-ring of the anthocyanin structure, while the other involves attacking the oxonium ion on the C-ring. These pathways contribute to the effective scavenging of free radicals, making anthocyanins potent antioxidants [36]. The utilization of packaging films with enhanced antioxidant properties holds great promise and effectiveness in prolonging the shelf life of food products. The incorporation of extracts abundant in hydroxyl groups into these films leads to heightened antioxidant activity. This, in turn, serves as a preventative measure against or decelerates the oxidation process in food products, thereby mitigating spoilage and extending the longevity of the packaged items (See Fig. 5.

Antibacterial activity of PVA/SC/PAE films

Antibacterial biodegradable films represent a novel paradigm shift in packaging technology. These revolutionary materials possess the dual advantage of inhibiting bacterial proliferation and readily decomposing in the environment. This remarkable combination offers a sustainable and impactful alternative to conventional plastic films, paving the way for a more eco-conscious future [46]. According to the data presented in Fig. 5A-B, the range of inhibition zone diameters against *S. typhimurium* for all tested samples was 0 to 12.16 mm. Similarly, the range of inhibition zone diameters against *S. aureus* was 0 to 9.12 mm. Among the tested films, the PVA/SC/PAE3 films exhibited the most effective broad-spectrum antibacterial activity, with inhibition zones measuring 12.16 mm for *S. typhimurium* and 9.12 mm for

Fig. 5 Antibacterial activity of PVA/SC, PVA/SC/PAE1, PVA/SC/PAE2 and PVA/SC/PAE3
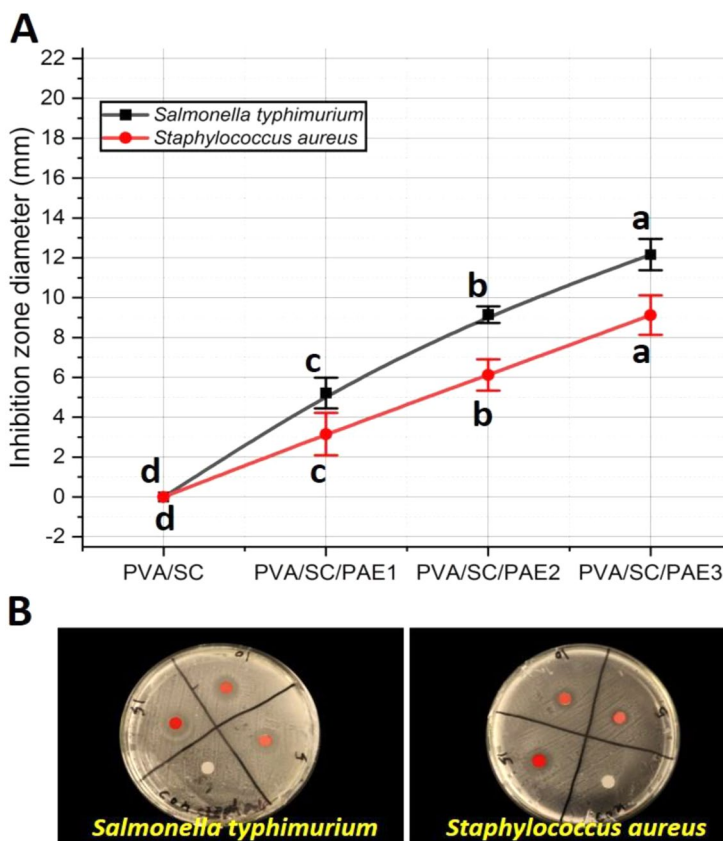
S. aureus. Therefore, the presence of PAE in the tested films resulted in the strongest inhibitory effect on bacterial growth. Anthocyanins have been discovered to possess antibacterial activity against a range of bacteria. Their mechanism of action is thought to involve multiple pathways. They have the ability to negatively impact the overall protein content and the activity of specific enzymes like alkaline phosphatase, adenosine triphosphatase, and superoxide dismutase in pathogenic bacteria [47]. The inclusion of nano active components within composite films has been demonstrated to effectively inhibit the growth of pathogenic bacteria during the shelf life of shrimp stored at 4 °C for a period of 6 days [48].

Physical, opacity and color properties of films

The incorporation of active components, such as PAE, into PVA/SC films can have an impact on the physical characteristics of the films. This experiment showcased these effects by assessing the thickness, solubility, swelling degree, and water vapor permeability (*WVP*) of the films. Table 2 demonstrates that increasing the concentrations of PAE in PVA/SC/PAE2-3 films led to a significant ($p < 0.05$) increase in film thickness. The highest thickness of 0.169 mm was observed in the PVA/SC/PAE3 film. An underlying reason for this observation could be a positive relationship between the concentration of anthocyanins and the thickness of the films. As the concentration of solids in the formulation increases, it directly affects the thickness of the films. Consequently, the presence of anthocyanins might have played a role in the observed increase in film thickness [12]. Moreover, plant extracts typically consist of large molecules that tend to aggregate and form a network-like structure within the film, thereby contributing to its increased thickness [49]. The findings presented in Table 2 indicate that with an increase in PAE concentration, both the swelling degree and solubility of the films increased. Notably, the PVA/SC/PAE3 film exhibited the highest values for swelling degree and solubility, reaching 45.14% and 27.15% respectively. The introduction of anthocyanins into the biodegradable films enhanced their solubility in water, likely due to an augmentation in the number of hydrophilic sites available for water absorption through interactions between PVA/SC and anthocyanins. [50]. The same manners were observed previously [51]. The enhanced ability of PVA/SC/PAE films to swell and exhibit semi-solubility is advantageous for our films as it facilitates rapid color release from the films into the product [52]. This characteristic also enables the effective transfer of natural multifunctional bioactive colorants to semi-moisture food products, contributing to their overall quality and appeal.

Table 2 physical, opacity and color properties of films

Parameters	Control films PVA/SC	Films with anthocyanins		
		PVA/SC/PAE1	PVA/SC/PAE2	PVA/SC/PAE3
Thickness (mm)	0.103 ± 0.001[c]	0.103 ± 0.002[c]	0.137 ± 0.001[b]	0.169 ± 0.003[a]
Solubility (%)	18.24 ± 0.72[d]	22.16 ± 0.91[c]	24.10 ± 0.82[b]	27.15 ± 0.43[a]
Swelling degree (%)	25.30 ± 0.90[d]	28.13 ± 0.58[c]	32.16 ± 0.90[b]	45.14 ± 0.69[a]
$WVP (\times 10^{-10} \text{g.m}^{-1}\text{s-1 pa}^{-1})$	1.652 ± 0.002[b]	1.641 ± 0.004[b]	1.021 ± 0.006[c]	1.876 ± 0.001[a]
Opacity	1.210 ± 0.210[d]	1.873 ± 0.220[c]	2.871 ± 0.310[b]	3.421 ± 0.410[a]
Color parameters				
L*	84.15 ± 0.621[a]	68.22 ± 0.70[b]	33.33 ± 0.81[c]	22.15 ± 0.68[d]
a*	-0.27 ± 0.04[d]	20.34 ± 0.21[c]	43.96 ± 0.72[b]	57.09 ± 0.31[a]
b*	0.07 ± 0.01[d]	18.93 ± 0.04[c]	30.09 ± 0.31[b]	41.10 ± 0.50[a]
Δ E	32.14 ± 0.31[d]	39.15 ± 0.14[c]	45.47 ± 1.02[b]	51.21 ± 0.87[a]

WVP = water vapor permeability, $L*$ = trend towards transparency, $a*$ = trend towards red, $b*$ = trend towards yellow and ΔE = total color difference

In Table 2, the WVP values for PVA/SC and PVA/SC/PAE films are provided. The study observed that the transfer rate of water vapor for PVA/SC films was 1.652×10^{-10} g.m^{-1} s^{-1} pa^{-1}. With an increase in the loading of PAE within PVA/SC/PAE2 films, there was a slight decrease in WVP to 1.021×10^{-10} g.m^{-1} s^{-1} pa^{-1} ($p < 0.05$). The decrease in WVP in bio-composite films can be explained by the intermolecular interactions, specifically hydrogen bonds, that occur between PVA/SC and PAE. These interactions result in an absorption of water vapor between films molecules with reduction in the movement or diffusion of water molecules within the film [24]. However, the continuous addition of PAE inside PVA/SC/PAE3 increased WVP to 1.876×10^{-10} g.m^{-1} s-1 pa^{-1}. The surface, internal cracks and crystalinity changes that occurred after using higher concentrations from PAE might explain evaporation of water vapour from films. The results of SEM and XRD proved the suggested explanation.

Analysis of Table 2 reveals notable disparities in the color indices and opacity of the film samples when different combinations of PVA/SC and PAE additives are utilized. Notably, as the concentration of PAE increases, the $L*$ value of the samples decreases. The highest $L*$ value of 84.15 is observed in the PVA/SC film, while the lowest $L*$ value of 22.15 is observed in the PVA/SC/PAE3 film.

Upon examination of the data, it can be observed that the $a*$ and $b*$ values of the film samples increase as the concentration of PAE rises. Particularly, the PVA/SC/PAE3 film exhibits the highest $a*$ value, indicating the transfer of the principal color of anthocyanins within the films. Moreover, the highest opacity value of 3.421 is observed in the PVA/SC/PAE3 film, while the lowest opacity value of 1.210 is observed in the PVA/SC film. These findings suggest that the inclusion of PAE in PVA/SC films results in the creation of opaque films with elevated $a*$, $b*$, and opacity values. This characteristic can be advantageous for preserving light-sensitive products, such as oily food products.

Application of PVA/SC/PAE on minced meat

The study analyzed the effects of using PVA/SC/PAE2 and PP as a wrapper material for minced meat during cold storage and un-covered (UC) meat was utilized as control. The color of minced meat and bio-transfer films were noticed during storage in Fig. 6A-C. Concerning the color of bio-films (Fig. 6A), it was cleared that the PVA/SC/PAE2 films showed a significant decrease in $a*$ value over time, indicating a loss of redness. Additionally, the PVA/SC/PAE2 films showed increase in $L*$ value over time, indicating that the films became lighter during storage. On the other hand, as illustrated in Fig. 6B, the color of minced meat changed during storage towards favorable redness color. This suggests that the films may interact with the meat in different ways and affect its color differently. Bio-transfer packaging films are a relatively new and exciting development in the packaging industry. They're designed to transfer beneficial bioactive compounds from the packaging material itself into the food product they contain.

The chemical indicators for minced meat freshness during cold storage were characterized through determination of pH, TVB-N and PV as indicated in Fig. 7A-C. The initial pH range (Fig. 7A) of fresh minced meat at the beginning was determined to be 5.4. Over a period of 5 days, there was an observed increase in the pH values of the uncovered (UC) samples and the samples wrapped with polypropylene (PP), reaching levels of 5.8 and 5.7, respectively. Subsequently, the pH values of the UC samples reached a maximum level of 6.4. In comparison, the samples covered with PVA/SC/PAE2 maintained stable pH values throughout the entire refrigeration period, with no significant differences observed. The elevation in pH observed in refrigerated meat during storage is likely attributed to increased bacterial growth and the breakdown of protein components [53]. On the other hand, the consistent pH stability observed in samples covered with PVA/SC/PAE2 can be attributed to the gradual release of anthocyanin components from the films into the meat samples, as depicted in Fig. 6. This release of
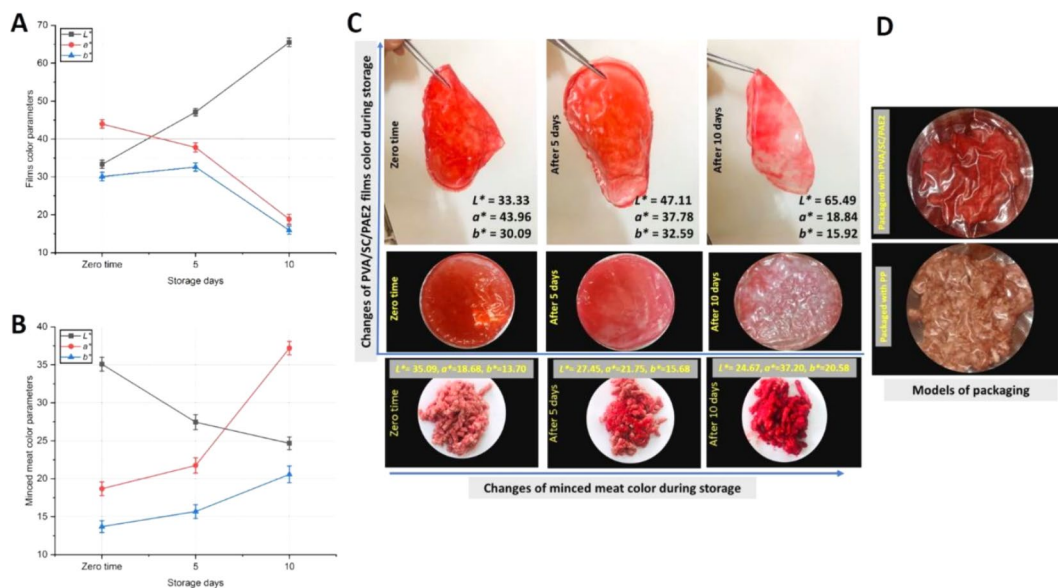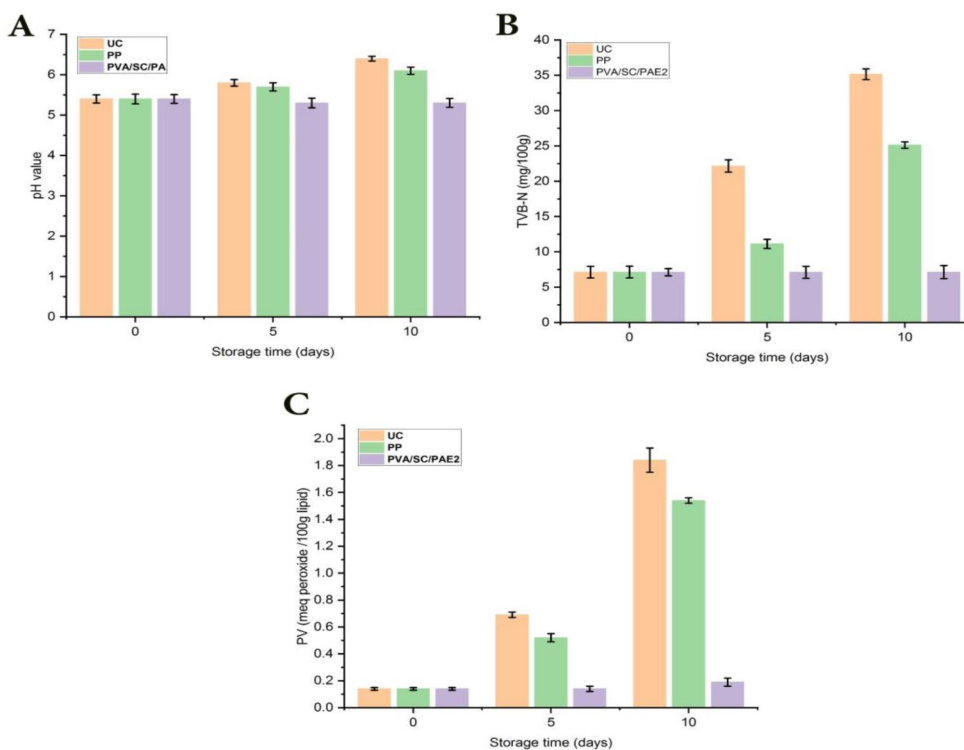
Fig. 6 Differences of Color properties of PVA/SC/PAE2 films (**A**), minced meat (**B**), real appearance of PVA/SC/PAE2 films and minced meat (**C**) and model of tested packaging (**D**) during cold storage

Fig. 7 Changes in pH value (A), TVB-N (B), and PV (C) of packaging minced meat during cold storage. UC = samples un covered and PP = samples covered with polypropylene

anthocyanins has the potential to inhibit the growth of foodborne pathogens [54].

TVB-N primarily originates from spoilage microorganisms and is commonly employed as an indicator for evaluating compounds containing ammonia, as well as primary, secondary, and tertiary amines. The initial TVB-N measurement of raw meat was determined to be 7.34 mg N/100 g,

indicating the freshness of the meat samples. As anticipated, the TVB-N values of the UC and PP meat samples exhibited a significant increase as the storage time increased ($p < 0.05$) Fig. 7B. At the end of storage time the TVB-N reached to 35.32 mg/100 g for UC samples and 25.22 mg/100 g for PP samples. On the other hand, the TVB-N values 7.34 mg N/100 g for PVA/SC/PAE2 were stable with non-significant

differences during storage time. One possible explanation for this stability is that the rapid reduction in the bacterial population of the meat samples may have diminished the ability of bacteria to undergo oxidative deamination of non-protein nitrogen compounds [55]. This reduction in bacterial activity could be attributed to the release of significant amounts of anthocyanins into the meat that was proven in Fig. 6, which may have contributed to the inhibition of bacterial growth.

The peroxide value (PV) of the meat samples stored under uncoated (UC) conditions, as well as samples coated with PP and PVA/SC/PAE2, is presented in Fig. 7C. After 10 days of cold storage, both the UC and PP packaged samples exhibited a noticeable increase in peroxide values. In contrast, the PVA/SC/PAE2 packaged samples demonstrated exceptional stability throughout the tested storage periods. Therefore, the utilization of active PVA/SC/PAE2 films may have positive effects on the oxidative stability of meat during storage. The observed results can be attributed to several possible explanations. Firstly, the presence of anthocyanins within the films resulted in the formation of opaque films, which effectively slowed down the oxidation process during the initial days of storage. This opacity likely facilitated the absorption or reflection of light, contributing to the deceleration of oxidation. Additionally, the active PVA/SC/PAE2 films gradually released a significant amount of potent antioxidants to the meat samples, effectively preventing the oxidation of the meat. Moreover, another potential benefit of the active PVA/SC/PAE2 films is their ability to inhibit the growth of psychrotrophic bacteria. These bacteria have the capability to produce lipase and phospholipase enzymes, which can lead to the release of short-chain fatty acids and subsequently contribute to increased oxidation during refrigerated meat storage. The presence of the active films may impede the growth of these bacteria, thereby reducing the production of these enzymes and minimizing the oxidation of the liberated fatty acids [56].

Conclusions

This research developed new bio-transfer films composed of PVA/SC and PAE. Incorporating up to 0.8% PAE into the PVA/SC films reduced their *WVP*, suggesting that these films are capable of maintaining a moderate moisture level around enclosed products. Moreover, the films demonstrated improved antioxidant and antibacterial properties, as well as increased opacity. These films effectively acted as bio-transfer layers, delivering active PAE to extend the shelf life of minced meat. The study found that using PVA/SC/PAE films for packaging minced meat helped maintain its quality during cold storage better than conventional

plastic packaging. Overall, the findings indicate that these biodegradable films hold potential for various food preservation applications, representing an innovative method for extending shelf life. The results of this research indicate that the developed technique, acting as an effective bio-transfer layer, has the potential to deliver colored active components. This approach offers an alternative to the excessive utilization of synthetic food preservatives. Also, this finding opens up possibilities for future applications aimed at enhancing food safety and quality while minimizing the use of synthetic additives.

Author contributions Mohamed Abdin: Conception and design of study, Data curation, formal analysis, conceptualization, methodology, resources, software, supervision, writing – original draft, investigation. Mohamed N. Saleh: Analysis and interpretation of data. Hazem Sakr: Data curation, formal analysis, conceptualization, methodology. Mohamed Elbana: Analysis, interpretation of data, drafting the manuscript. Reham M. Kamel: Writing – original draft, revising the manuscript critically for important intellectual content. Mohamed M. El-kholy: Writing – original draft, revising the manuscript critically for important intellectual content. Enas El. Fadly: Acquisition of data. Mohamed Abdelbaset Salama: Methodology conceptualization, data curation, formal analysis.

Data availability Data will be made available on reasonable request.

Declarations

Competing interest The authors declared that they have no conflict of interest.

References

1. Z. Yu, Q. Jiang, D. Yu, J. Dong, Y. Xu, W. Xia, Physical, antioxidant, and preservation properties of chitosan film doped with proanthocyanidins-loaded nanoparticles. Food Hydrocoll. 2022(Sep.):130

2. L. Mei, Q. Wang, Advances in using nanotechnology structuring approaches for improving Food Packaging. Annual Rev. Food Sci. Technol. **11**(1), – (2020)

3. O.F.J.G. De, M.G.M.N. De, M.R.V. Bertolo, M.A.V. Rodrigues, J.S. Bogusz, G.D.C. Silva et al., Recent advances in the development of smart, active, and bioactive biodegradable biopolymer-based films containing betalains. Food Chem. 2022(Oct.1):390

4. X. Zhang, Y. Liu, H. Yong, Y. Qin, J. Liu, J. Liu, Development of multifunctional food packaging films based on chitosan, TiO2 nanoparticles and anthocyanin-rich black plum peel extract. Food Hydrocoll. **94**(SEP), 80–92 (2019)

5. H. Abral, A. Atmajaya, M. Mahardika, F. Hafizulhaq, D. Handayani, S. Sapuan et al., Effect of ultrasonication duration of polyvinyl alcohol (PVA) gel on characterizations of PVA film. J. Mater. Res. Technol. **9**(2), 2477–2486 (2020)

6. P.S. Premkumar, Preparation and electrical studies on pure and oxygen plasma treated polyvinyl alcohol films. J. Mater. Res. Technol. **8**(2), 2232–2237 (2019)

7. M. Alizadeh-Sani, J.-W. Rhim, M. Azizi-Lalabadi, M. Hemmati-Dinarvand, A. Ehsani, Preparation and characterization of functional sodium caseinate/guar gum/TiO2/cumin essential oil composite film. Int. J. Biol. Macromol. **145**, 835–844 (2020)

8. K.-K. Li, S.-W. Yin, X.-Q. Yang, C.-H. Tang, Z.-H. Wei, Fabrication and characterization of novel antimicrobial films derived from thymol-loaded zein–sodium caseinate (SC) nanoparticles. J. Agric. Food Chem. **60**(46), 11592–11600 (2012)

9. S. Paidari, N. Zamindar, R. Tahergorabi, M. Kargar, S. Ezzati, N. Shirani et al., Edible coating and films as promising packaging: a mini review. J. Food Meas. Charact. **15**(5), 4205–4214 (2021)

10. S. Sheibani, S. Jafarzadeh, Z. Qazanfarzadeh, M.M.J. Osadee Wijekoon, N.H. Mohd Rozalli, A. Mohammadi Nafchi, Sustainable strategies for using natural extracts in smart food packaging. Int. J. Biol. Macromol. **267**, 131537 (2024). https://doi.org/10.1016/j.ijbiomac.2024.131537

11. A. Chanoca, N. Kovinich, B. Burkel, S. Stecha, A. Bohorquez-Restrepo, T. Ueda et al., Anthocyanin Vacuolar inclusions Form by a Microautophagy mechanism. Plant. Cell. 2015

12. L. Prietto, T.C. Mirapalhete, V.Z. Pinto, J.F. Hoffmann, N.L. Vanier, L.T. Lim et al., pH-sensitive films containing anthocyanins extracted from black bean seed coat and red cabbage. LWT-Food Sci. Technol. **80**, 492–500 (2017)

13. J. Moustaka, E. Panteris, I.D.S. Adamakis, G. Tanou, A. Giannakoula, E.P. Eleftheriou et al., *High Anthocyanin Accumulation in poinsettia Leaves is Accompanied by Thylakoid Membrane Unstacking, Acting as a Photoprotective Mechanism, to Prevent ROS Formation* (Environmental & Experimental Botany, 2018), p. S0098847218300546

14. F. Alnadari, S. Al-Dalali, F. Pan, M. Abdin, E.B. Frimpong, Z. Dai et al., Physicochemical characterization, molecular modeling, and applications of carboxymethyl chitosan-based multifunctional films combined with gum arabic and anthocyanins. Food Bioprocess Technol. **16**(12), 2984–3002 (2023)

15. A.A. Alshehri, Y.S. Hamed, R.M. Kamel, S.M. Shawir, H. Sakr, M. Ali et al., Enhanced physical properties, antioxidant and antibacterial activity of bio-composite films composed from carboxymethyl cellulose and polyvinyl alcohol incorporated with broccoli sprout seed extract for butter packaging. Int. J. Biol. Macromol. 2023:128346

16. P. Kraisit, M. Luangtana-Anan, N. Sarisuta, Effect of various types of Hydroxypropyl Methylcellulose (HPMC) films on Surface Free Energy and Contact Angle. Adv. Mater. Res. **1060**, 107–110 (2015)

17. H. Du, C. Liu, O. Unsalan, C. Altunayar-Unsalan, S. Xiong, A. Manyande et al., Development and characterization of fish myofibrillar protein/chitosan/rosemary extract composite edible films and the improvement of lipid oxidation stability during the grass carp fillets storage. Int. J. Biol. Macromol. **184**, 463–475 (2021)

18. M. Jouki, F.T. Yazdi, S.A. Mortazavi, A. Koocheki, N. Khazaei, Effect of quince seed mucilage edible films incorporated with oregano or thyme essential oil on shelf life extension of refrigerated rainbow trout fillets. Int. J. Food Microbiol. **174**, 88–97 (2014)

19. A.F. Faria, M.C. Marques, A.Z. Mercadante, Identification of bioactive compounds from jambolão (Syzygium cumini) and antioxidant capacity evaluation in different pH conditions. Food Chem. **126**(4), 1571–1578 (2011)

20. C. Jampani, A. Naik, K.S.M.S. Raghavarao, Purification of anthocyanins from jamun (Syzygium cumini L.) employing adsorption. Sep. Purif. Technol. **125**, 170–178 (2014)

21. S. Hanju, Pingping, Zhang, Yongsheng, Zhu et al., Antioxidant and prebiotic activity of five peonidin-based anthocyanins extracted from purple sweet potato (Ipomoea batatas (L.) Lam.). Sci. Rep. 2018

22. N. Chorfa, S. Savard, K. Belkacemi, An efficient method for high-purity anthocyanin isomers isolation from wild blueberries and their radical scavenging activity. Food Chem. **197**, 1226–1234 (2016). APR.15PT.B)

23. Y. Xu, D. Hu, Y. Li, C. Sun, W. Chen, *An Effective Method for Preparation of high-purity Pelargonidin-3-O-glucoside from Strawberry and its Protective Effect on Cellular Oxidative Stress* (JOURNAL OF CHROMATOGRAPHY B, 2018)

24. F. Alnadari, S. Al-Dalali, F. Pan, M. Abdin, E.B. Frimpong, Z. Dai et al., Physicochemical characterization, molecular modeling, and applications of Carboxymethyl Chitosan-based multifunctional films combined with Gum Arabic and anthocyanins. Food Bioprocess Technol. 2023:1–19

25. I. Korbag, S. Mohamed Saleh, Studies on the formation of intermolecular interactions and structural characterization of polyvinyl alcohol/lignin film. Int. J. Environ. Stud. **73**(2), 226–235 (2016)

26. G.J.C. Fernandes, P.H. Campelo, de J. Abreu Figueiredo, H.J. Barbosa de Souza, M.R.S. Peixoto Joele, M.I. Yoshida et al., Effect of polyvinyl alcohol and carboxymethylcellulose on the technological properties of fish gelatin films. Sci. Rep. **12**(1), 10497 (2022)

27. M.M. Gomaa, E.E. Fadly, M.A. Salama, M. Abdin, Production of bio-composite films from gum arabic and galangal extract to prolong the shelf life of Agaricus Bisporus. J. Polym. Environ. **30**(11), 4787–4799 (2022)

28. L. Wang, H. Guo, J. Wang, G. Jiang, F. Du, X. Liu, Effects of Herba Lophatheri extract on the physicochemical properties and biological activities of the chitosan film. Int. J. Biol. Macromol. **133**, 51–57 (2019)

29. A. Riaz, C. Lagnika, H. Luo, Z. Dai, M. Nie, M.M. Hashim et al., Chitosan-based biodegradable active food packaging film

containing Chinese chive (Allium tuberosum) root extract for food application. Int. J. Biol. Macromol. **150**, 595–604 (2020)

30. B.U. Chaudhary, S. Lingayat, A.N. Banerjee, R.D. Kale, Development of multifunctional food packaging films based on waste garlic peel extract and Chitosan. Int. J. Biol. Macromol. **192**, 479–490 (2021)

31. S. Pourjavaher, H. Almasi, S. Meshkini, S. Pirsa, E. Parandi, Development of a colorimetric pH indicator based on bacterial cellulose nanofibers and red cabbage (Brassica Oleraceae) extract. Carbohydr. Polym. **156**, 193–201 (2017)

32. da J.C.M. Costa, K.S.L. Miki, da A. Silva Ramos, B.E. Teixeira-Costa, Development of biodegradable films based on purple yam starch/chitosan for food application. Heliyon 2020;**6**(4)

33. S. Pokhrel, A. Sigdel, R. Lach, M. Slouf, J. Sirc, V. Katiyar et al., Starch-based biodegradable film with poly (butylene adipate-co-terephthalate): Preparation, morphology, thermal and biodegradation properties. J. Macromolecular Sci. Part A **58**(9), 610–621 (2021)

34. S. Collazo-Bigliardi, R. Ortega-Toro, A.C. Boix, Isolation and characterisation of microcrystalline cellulose and cellulose nanocrystals from coffee husk and comparative study with rice husk. Carbohydr. Polym. **191**, 205–215 (2018)

35. F. Alnadari, S. Al-Dalali, M.M. Nasiru, E.B. Frimpong, Y. Hu, D. Abdalmegeed et al., A new natural drying method for food packaging and preservation using biopolymer-based dehydration film. Food Chem. **404**, 134689 (2023)

36. S. Wang, P. Xia, S. Wang, J. Liang, Y. Sun, P. Yue et al., Packaging films formulated with gelatin and anthocyanins nanocomplexes: physical properties, antioxidant activity and its application for olive oil protection. Food Hydrocoll. **96**, 617–624 (2019)

37. M. Abdin, M. Mabrouk, L. El-Sebaiy, M. Eissa, M. El-Bana, M.A. Salama et al., Composite films based on carboxy methyl cellulose and sodium alginate incorporated Thymus vulgaris purified leaves extract for food application: Assessment, antimicrobial and antioxidant properties. Int. J. Biol. Macromol. **240**, 124474 (2023)

38. R. Bidari, A.A. Abdillah, R.A.B. Ponce, A.L. Charles, Characterization of biodegradable films made from Taro Peel (Colocasia esculenta) starch. Polymers. **15**(2), 338 (2023)

39. S. Forghani, F. Zeynali, H. Almasi, H. Hamishehkar, Characterization of electrospun nanofibers and solvent-casted films based on Centaurea Arvensis anthocyanin-loaded PVA/κ-carrageenan and comparing their performance as colorimetric pH indicator. Food Chem. **388**, 133057 (2022)

40. D. Liu, Z. Cui, M. Shang, Y. Zhong, A colorimetric film based on polyvinyl alcohol/sodium carboxymethyl cellulose incorporated with red cabbage anthocyanin for monitoring pork freshness. Food Packaging Shelf Life. **28**, 100641 (2021)

41. X. Zhai, J. Shi, X. Zou, S. Wang, C. Jiang, J. Zhang et al., Novel colorimetric films based on starch/polyvinyl alcohol incorporated with roselle anthocyanins for fish freshness monitoring. Food Hydrocoll. **69**, 308–317 (2017)

42. C. Pastor, L. Sánchez-González, A. Chiralt, M. Cháfer, C. González-Martínez, Physical and antioxidant properties of chitosan and methylcellulose based films containing resveratrol. Food Hydrocoll. **30**(1), 272–280 (2013)

43. A. Riaz, C. Lagnika, H. Luo, M. Nie, Z. Dai, C. Liu et al., Effect of Chinese chives (Allium tuberosum) addition to carboxymethyl cellulose based food packaging films. Carbohydr. Polym. **235**, 115944 (2020)

44. F. Alnadari, A.P. Bassey, M. Abdin, M.A. Salama, M.M. Nasiru, Z. Dai et al., Development of hybrid film based on carboxymethyl chitosan-gum arabic incorporated citric acid and polyphenols from Cinnamomum camphora seeds for active food packaging. J. Polym. Environ. **30**(9), 3582–3597 (2022)

45. C. Ballester-Costa, E. Sendra, J. Fernández-López, M. Viuda-Martos, Evaluation of the antibacterial and antioxidant activities of chitosan edible films incorporated with organic essential oils obtained from four Thymus species. J. Food Sci. Technol. **53**, 3374–3379 (2016)

46. E. Hernández-García, M. Vargas, C. González-Martínez, A. Chiralt, Biodegradable antimicrobial films for food packaging: Effect of antimicrobials on degradation. Foods. **10**(6), 1256 (2021)

47. X.-. Sun, T.-. Zhou, C.-. Wei, W.-. Lan, Y. Zhao, Y.-. Pan et al., Antibacterial effect and mechanism of anthocyanin rich Chinese wild blueberry extract on various foodborne pathogens. Food Control. **94**, 155–161 (2018)

48. S. Paidari, H. Ahari, The effects of nanosilver and nanoclay nanocomposites on shrimp (Penaeus semisulcatus) samples inoculated to food pathogens. J. Food Meas. Charact. **15**(4), 3195–3206 (2021)

49. E. Sogut, A.C. Seydim, The effects of Chitosan and grape seed extract-based edible films on the quality of vacuum packaged chicken breast fillets. Food Packaging Shelf Life. **18**, 13–20 (2018)

50. T. Borkowski, H. Szymusiak, A. Gliszczyńska-Swigo, B. Tyrakowska, The effect of 3-O-β-glucosylation on structural transformations of anthocyanidins - ScienceDirect. Food Res. Int. **38**(8–9), 1031–1037 (2005)

51. F. Garavand, Application of Red Cabbage Anthocyanins as pH-Sensitive pigments in Smart Food Packaging and Sensors. Polymers 2022;**14**

52. Y. Zhong, A colorimetric film based on polyvinyl alcohol/sodium carboxymethyl cellulose incorporated with red cabbage anthocyanin for monitoring pork freshness. Food Packaging Shelf Life 2021;**28**(5)

53. R.Y. Hao, L.M. Liu, Sun, Xia et al., Sodium alginate coating with plant extract affected microbial communities, biogenic amine formation and quality properties of abalone (Haliotis discus hannai Ino) during chill storage. LWT-FOOD SCI. TECHNOL. **2017**(–), 1–9 (2017)

54. Y. Ma, S. Ding, Y. Fei, G. Liu, J. Fang, Antimicrobial activity of anthocyanins and catechins against foodborne pathogens Escherichia coli and Salmonella. Food Control. **106**, 106712 (2019)

55. N. Shavisi, A. Khanjari, A.A. Basti, A. Misaghi, Y. Shahbazi, Effect of PLA films containing propolis ethanolic extract, cellulose nanoparticle and ziziphora clinopodioides essential oil on chemical, microbial and sensory properties of minced beef. Meat Sci. **124**(FEB), 95–104 (2017)

56. N.P. Nirmal, S. Benjakul, Retardation of quality changes of Pacific white shrimp by green tea extract treatment and modified atmosphere packaging during refrigerated storage. Int. J. Food Microbiol. **149**(3), 247–253 (2011)